Plant Physiology and Biochemistry 141 (2019) 60–72

Contents lists available at ScienceDirect

Plant Physiology and Biochemistry

journal homepage: www.elsevier.com/locate/plaphy

Research article

A functional homologue of *Arabidopsis TTG1* from *Freesia* interacts with bHLH proteins to regulate anthocyanin and proanthocyanidin biosynthesis in both *Freesia hybrida* and *Arabidopsis thaliana*

Xiaotong Shan[a], Yueqing Li[a], Song Yang[a], Ruifang Gao[a], Liudi Zhou[a], Tingting Bao[a], Taotao Han[a], Shucai Wang[a], Xiang Gao[a,b,*], Li Wang[a,**]

[a] Key Laboratory of Molecular Epigenetics of MOE and Institute of Genetics & Cytology, Northeast Normal University, Changchun, China
[b] National Demonstration Center for Experimental Biology Education, Northeast Normal University, Changchun, China

ARTICLE INFO

Keywords:
Anthocyanin biosynthesis
Proanthocyanidin biosynthesis
WD40 protein
MBW complex
Trichome formation

ABSTRACT

The MBW complex, consisting of MYB, basic helix-loop-helix (bHLH) and WD40 proteins, regulates multiple traits in plants, such as anthocyanin and proanthocyanidin biosynthesis and cell fate determination. The complex has been widely identified in dicot plants, whereas few studies are concentrated on monocot plants which are of crucial importance to decipher its functional diversities among angiosperms during evolution. In present study, a WD40 gene from *Freesia hybrida*, designated as *FhTTG1*, was cloned and functionally characterized. Real-time PCR analysis indicated that it was expressed synchronously with the accumulation of both proanthocyanidins and anthocyanins in *Freesia* flowers. Transient protoplast transfection and biomolecular fluorescence complementation (BiFC) assays demonstrated that FhTTG1 could interact with FhbHLH proteins (FhTT8L and FhGL3L) to constitute the MBW complex. Moreover, the transportation of FhTTG1 to nucleus was found to rely on FhbHLH factors. Outstandingly, FhTTG1 could highly activate the anthocyanin or proanthocyanidin biosynthesis related gene promoters when co-transfected with MYB and bHLH partners, implying that FhTTG1 functioned as a member of MBW complex to control the anthocyanin or proanthocyanidin biosynthesis in *Freesia hybrida*. Further ectopic expression assays in *Arabidopsis ttg1-1* showed the defective phenotypes of *ttg1-1* were partially restored. Molecular biological assays validated FhTTG1 might interact with the endogenous bHLH factors to up-regulate genes responsible for anthocyanin and proanthocyanidin biosynthesis and trichome formation, indicating that FhTTG1 might perform exchangeable roles with AtTTG1. These results will not only contribute to the characterization of FhTTG1 in *Freesia* but also shed light on the establishment of flavonoid regulatory system in monocot plants, especially in *Freesia hybrida*.

1. Introduction

Plants are thought to have colonized the land niche since around 400 million years ago and then developed a range of strategies to survive in the new habitats, among which the evolutionary emergences of the flavonoids and trichomes are considered to enable the adaptation of plants in the complex and versatile land environment (Davies et al., 2012; Schiestl and Johnson, 2013; Sobel and Streisfeld, 2013; Waters, 2003). Typically, flavonoid biosynthesis and trichome formation on stems have been hypothesized to contribute to the synergetic defenses against damages caused by UV light irradiation and predators foraging, respectively (Pesch et al., 2015; Serna et al., 2006; Stapleton and Walbot, 1994).

Elucidating the genetic basis of the physiological adaptations has benefits to understand the evolutionary processes. It has been well established that the transcriptional regulation of flavonoid biosynthesis (e.g. anthocyanin and proanthocyanidin biosynthesis) and cell fate determination (e.g. trichome formation) is controlled by DNA-binding R2R3 MYB regulators, basic helix–loop–helix (bHLH) factors, and WD40 proteins (designated as MBW complex) (Hichri et al., 2011; Passeri et al., 2016; Xu et al., 2015; Zhao et al., 2012; Zhou et al., 2014). Virtually, the MBW complex is also implemented in other physiological processes, e.g., seed coat mucilage production (Gonzalez et al., 2009; Ranocha et al., 2014; Zhao et al., 2012; Zheng et al., 2016).

* Corresponding author. Key Laboratory of Molecular Epigenetics of MOE and Institute of Genetics & Cytology, Northeast Normal University, Changchun, China.
** Corresponding author.
E-mail addresses: gaoxiang424@163.com (X. Gao), wanglee57@163.com (L. Wang).

https://doi.org/10.1016/j.plaphy.2019.05.015
Received 7 September 2018; Received in revised form 22 April 2019; Accepted 15 May 2019
Available online 20 May 2019
0981-9428/

In general, MYB proteins are regarded as the dominant components to determine target genes of MBW complexes, while the bHLH proteins belonging to subgroup IIIf have been found to exert partial and somehow overlapping roles in several branches of the flavonoid pathway (Koes et al., 2005; Verweij et al., 2016). In addition, bHLH proteins also perform versatile roles in other physiological events such as trichome formation on *Arabidopsis* leaves (Payne et al., 2000). In contrast, WD40 proteins without transactivation capacities are expressed more or less ubiquitously and can be indulged in most of the physiological and metabolic events aforementioned (Nocker and Ludwig, 2003). Based on the previous studies, special attention was mainly focused on MYB and bHLH regulators in plant kingdom, ranging from spermatophytes to mosses. There are also a few WD40 proteins functionally characterized in dicotyledons to be indispensable for the biosynthesis of anthocyanin or proanthocyanidin and trichome formation, including AN11 from *Petunia* (De et al., 1997), TTG1 from *Arabidopsis* (Walker et al., 1999), PFWD from *Perilla* (Sompornpailin et al., 2002), ZmPAC1 from Maize (Carey and Chandler, 2004), MtWD40-1 from *Medicago* (Pang et al., 2009), WDR1 and WDR2 from Grapevine (Matus et al., 2010), PgWD40 from Pomegranate (Zohar et al., 2011), MdTTG1 from Apple (An et al., 2012) and DkWDR1 from Persimmon (Naval et al., 2016). Comparably, few WD40 regulators have been experimentally proved to be involved in aforementioned events in monocot plants (Carey and Chandler, 2004).

Freesia hybrida, one monocotyledonous horticultural plant in Iridaceae, is prestigious for its colorful flowers ranging from white to purple. In addition, the flowers also showed intricate floral pigmentation patterns such as petal blushing, flecks and venation. Our previous studies have shown that anthocyanins, proanthocyanidins and flavonols could be simultaneously synthesized in the flowers of *Freesia* cultivar, Red River®, indicating a complicated but ordered regulatory network finely regulating the flavonoid biosynthesis (Li et al., 2016; Sun et al., 2015). Recently, one MYB factor gene *FhMYB5* and seven structural genes including *FhCHS1*, *FhDFR1*, *FhDFR2*, *FhDFR3*, *Fh3GT1*, *Fh5GT1* and *Fh5GT2*, have been isolated and characterized to function in flavonoid biosynthesis in Red River® (Ju et al., 2018; Li et al., 2017, 2019; Sui et al., 2011; Sun et al., 2015, 2016, 2017). Moreover, two bHLH regulators, FhGL3L and FhTT8L, were also functionally proved to participate in flavonoid biosynthesis and trichome formation (Li et al., 2016). However, no WD40 proteins to our knowledge have been reported in *Freesia* yet, which deserves further concerns considering its versatile roles in several metabolic pathways.

In this study, a sequence encoding potential WD40 protein was mined from the former constructed *Freesia* transcriptomic database and tentatively designated as *FhTTG1*. The temporal and spatial expression of *FhTTG1* coincided well with anthocyanin and proanthocyanidin accumulations in *Freesia* flowers. BiFC analysis demonstrated that FhTTG1 could interact with FhTT8L or FhGL3L to form complex and then be imported into the nucleus interdependently or synergistically. Transient expression in *Freesia* protoplast illustrated that *FhTTG1* might function as a member of *Freesia* MBW complex in regulating anthocyanin or proanthocyanidin related genes *in vivo*. In addition, ectopic expression of *FhTTG1* in *Arabidopsis* could partially complement the phenotypes of *ttg1* mutant. Further transient protoplast transfection assays suggested the exchangeable roles between *Freesia TTG1* and *Arabidopsis TTG1*. In conclusion, the functionality of WD40 protein FhTTG1 was firstly verified and the results here lay ground for further deciphering the regulatory mechanisms of flavonoid biosynthesis in *Freesia hybrida*.

2. Materials and methods

2.1. Plant materials and growth conditions

The *Freesia hybrida* with red flowers (Red River®) was cultivated in sandy loam with pH 6.5–7.2 in greenhouse under 14 h/10 h (light/dark) photoperiod, and the temperature was set at 25 °C in the light and 15 °C in the dark. The flower development process was divided into 5 stages according to pigmentation status. The flowers at the fifth stage were further divided into 5 tissues, i.e. petal, calyx, torus, stamen and pistil. They were individually collected with 3 vegetative tissues, i.e. scape, leave and root (Gao et al., 2018; Li et al., 2016, 2017; Sun et al., 2015). All of the samples were put into the liquid nitrogen immediately and stored at −80 °C before use.

The young inflorescences containing flower stalks (3–4 cm) and kelly green flower buds were used to induce callus (Uwagaki et al., 2015; Wang et al., 1990). Briefly, young inflorescences were sterilized with sterilization solution containing 50% (v/v) hypochlorite solution and 0.01% (v/v) Tween 20 for 2–3 min, and then rinsed in sterile water four times. Subsequently, they were cut into ca. 2–3 mm thick cubes before transferred onto MS medium (Murashige and Skoog, 1962) supplemented with 1 mg L^{-1} thidiazuron (TDZ), 1 mg L^{-1} dicamba, 3% sucrose and 0.6% agar. The medium were adjusted to pH 5.8 and autoclaved at 116 °C for 30 min. The explants were incubated for callus regeneration in a growth chambers at 25 °C with 16 h light and 8 h dark period. And the photon flux density was set at 1800 lux. The pale-yellow nodular calluses were used for the protoplasts isolation.

The 5 to 6-week-old *Arabidopsis* grown in a growth chamber at 22 °C with 16 h light and 8 h dark was used for plant transformation. Seeds of Landsberg-0 (Ler-0) ecotypic, *ttg1-1* mutant (ABRC stock number: CS89) and homozygous transgenic plants were surface-sterilized by sodium hypochlorite, and germinated on 1/2 MS medium (Murashige and Skoog, 1962) with 3% w/v sucrose. About 6-day-old seedlings were harvested for further investigating the flavonoid accumulation and gene expression levels. A proportion of seedlings were then transplanted from the medium to soil for the trichomes observation. 3–4 weeks old *Arabidopsis* leaves of wild type (Columbia-0) were used for protoplasts isolation.

2.2. DNA and RNA extraction and cDNA synthesis

Freesia flowers were collected to extract the genomic DNA using NuClean Plant Genomic DNA Kit (CWBIO, Beijing, China) referring to the manufacturer's instruction. The OminiPlant RNA Kit (CWBIO, Beijing, China) was applied in the extraction of RNA from different samples of *Freesia* and *Arabidopsis* following the manufacturer's standard protocol. After DNaseI digestion, 1 μg of RNA was subsequently submitted to cDNA synthesis using Oligo $d(T)_{15}$ primers combined with M-MLV Reverse Transcriptase (Promega, Madison, WI) according to the manufacturer's instruction.

2.3. Sequence analysis

Multiple amino acid sequence alignment was carried out using Clustal Omega (Sievers et al., 2011). The entire amino acid sequence of FhTTG1 protein was further aligned with its orthologs from other plant species by Clustal Omega with default parameters. Subsequently, the alignments were subjected to MEGA version 6 to generate the neighbor-joining phylogenetic tree (Tamura et al., 2013). 1000 replicates were set as the bootstrapping number and the handling gaps way was pair wise deletion.

2.4. qRT-PCR analysis

SYBR Master Mix (TOYOBO, Osaka, Japan) was selected to perform the quantative real-time PCR analysis with the specific qRT-PCR primers designed and listed in Supplementary Table S1. The standard two-step PCR program was described in our earlier studies (Li et al., 2016, 2017). The Ct values of each gene were normalized to *18S rRNA* in *Freesia* and *Actin* in *Arabidopsis*, respectively (Li et al., 2016, 2017; Sun et al., 2016). The gene expression levels were determined with formula $2^{-\Delta\Delta C_T}$ (Livak and Schmittgen, 2001), and all biological replicates were

analyzed in triplicate.

2.5. Constructs engineering

To isolate the candidate genes, the entire amino acid sequence of AtTTG1 (Accession number: NM180738.3) was employed as bait sequence to screen the *Freesia* transcriptomic database (Li et al., 2016). After manual BLASTX search of National Center for Biotechnology Information (NCBI), a putative WD40 sequence with best hit was found. Then, specific primers were designed based on the predicted cDNA sequences and a routine PCR was carried out to amplify the *TTG1* like sequence from *Freesia* flowers (Table S1). PCR product of appropriate length was sequenced after being connected into pGEM-Teasy vector (Promega, Madison, WI) and then transformed into the *E. coli* JM109 competent cells.

The Minerva Super Fusion Cloning Kit (US Everbright® Inc., Suzhou, PRC) was employed in the following vector constructions. HA (Human influenza hemagglutinin) or GD (*GAL4* DNA binding domain)-tagged FhTTG1 were generated by fusing the N-terminus of FhTTG1 to the HA or GD tag under the control of the constitutive *CaMV* (cauliflower mosaic virus) *35S* promoter in the pUC19 backbone. Moreover, two copies of VP16 (a strong activation domain) were assembled to FhTTG1 by substituting the termination codon of FhTTG1 to generate HA or GD-tagged FhTTG1-VP16 (2 ×).

For *Arabidopsis* transformation, the HA tagged FhTTG1 vector was digested by *Eco*R I and the fragments were cloned into the binary vector pPZP211 by T_4 DNA ligase (TransGen Biotech, Beijing, China). The binary vectors were then introduced into *Agrobacterium tumefaciens* GV3101 strain for plant transformation.

To verify whether FhTTG1 participated in the activation of anthocyanin or proanthocyanidin genes, promoters of *FhDFR3*, *FhLDOX1* and *Fh3GT1* was amplified using Genome Walking Kit (Takara, Dalian, China) following the instructions, and *AtBAN* (Accession number: AT1G61720) promoter was cloned from *Arabidopsis thaliana* (Col-0) by specific primers retrieved from the corresponding genomic sequences (Table S1). The corresponding promoter sequences were cloned into *Pst*I and *Sac*I digested *DFR-*A_{pro}*:GUS* (beta-glucuronidase) vector which was described in earlier studies (Li et al., 2016).

For BiFC assays, GFP (green fluorescent protein) was splited into the truncated 174 residues of N-terminus (GFPN) and the truncated 66 residues of C-terminus (GFPC) by routine PCR. PCR products were submitted to substitute the HA tag in the modified pUC19 vector harboring *CaMV 35S* promoter and *NOS* terminator. The full-length region of *FhGL3L/FhTT8L* and *FhTTG1* were generated by PCR and subsequently inserted in frame into the *35S:GFPN* and *35S:GFPC* vectors to generate *35S:GFPN/GFPC-FhGL3L/FhTT8L*; *35S:GFPN/GFPC-FhTTG1* and *35S:GFPN-AtGL3/AtTT8*, respectively.

For intracellular localization assays, the *35S:FhTTG1/FhTT8L/FhGL3L-GFP* vectors were generated by replacing the gene termination codon with *GFP*. Otherwise, the *35S:GFP-FhTTG1/FhTT8L/FhGL3L* vectors were also constructed by fusing the GFP to the N-terminus of each protein. Besides, other constructs or primers employed in present study have been reported in our previous studies (Li et al., 2016, 2017; 2019; Wang et al., 2015).

2.6. Protoplast transfection, GUS activity, BiFC and intracellular localization assays

Protoplast preparation, transfection and GUS activity analysis were carried out as described earlier (Wang et al., 2015; Wang and Chen, 2008; Zhou et al., 2014). In brief, all the plasmids involved in protoplast transfection assays were extracted and purified by using GoldHi EndoFree Plasmid Maxi Kit (CWBIO, Beijing, China) following the standard protocol. A 10 μg aliquot of each plasmid was used in transfection assays. GD or CAT (chloramphenicol acetyltrasferase) plasmid DNA was used to equalize the amount of DNA wherever required (Wang and Chen, 2008). 3 to 4-week-old *Arabidopsis* rosette leaves were cut into pieces and subjected to protoplasts isolation by enzymolysis. The protoplasts were then transfected by constructs in the presence of polyethylene glycol 3350. GUS activity, BiFC and intracellular localization were analyzed after 21 h incubation under darkness at room temperature. GUS activities were measured by a SynergyTM HT microplate reader (BioTEK, www.biotek.com). BiFC and intracellular localization were visualized by fluorescence microscopy. GFP was observed with the filter BP450-490 (blue light) and RFP was observed with the filter BP546 (yellow light) (Wan et al., 2002).

The transient *Freesia* protoplast transfection assays were performed following the methods aforementioned with some modifications (Li et al., 2019). Briefly, 1 g of calluses were cut into millet-like fragments and then transferred into 15–18 mL enzyme solution containing 1% (w/v) of Cellulase R10 (Yakult Pharmaceutical Ind. Co., Ltd., Japan) and 0.75% (w/v) of Macerozyme R10 (Yakult Pharmaceutical Ind. Co., Ltd., Japan). The solution was incubated for 6 h on a shaker at 40 rpm at 22 °C in darkness. All the transfection assays were performed in triplicate and each experiment was repeated at least twice.

2.7. Plant transformation

About 5 to 6-week-old *Arabidopsis ttg1-1* mutants were transformed by *FhTTG1* gene driven by *CaMV 35S* promoter following the floral dip method (Bent, 2006). The harvested T1 seeds of transformed plants were sown on 1/2 MS medium supplemented with 50 mg L^{-1} kanamycin. After kanamycin selection, about 50 T1 kanamycin resistant plants were transferred to soil. After 3 weeks, one piece of rosette leaves of each line was used to extract RNA and investigated by RT-PCR (Fig. S1). According to the results, positive lines were kept to harvest T2 seeds, and then T2 seeds with recovered brown seed coats were selected to be sown on the medium with kanamycin. About 10 days later, T2 seedlings consistent with the 3:1 segregation ratio of green plants to albino plants were remained to gain the homozygous seeds. The homozygous seeds of at least 15 transgenic lines recovered the brown colors in their seed coats and one of which was selected for further analysis. The seeds were germinated and cultivated on 1/2 Murashige and Skoog (MS) medium containing 3% (w/v) sucrose for further analysis.

2.8. Anthocyanin and proanthocyanidin analysis

Total anthocyanin accumulation was quantified as described by Pandey (Pandey et al., 2014). Briefly, 300 mg of *Freesia* flower materials or 7-day-old *Arabidopsis* seedlings cultivated on 1/2 MS medium were ground thoroughly in liquid nitrogen. The powder was then dissolved and kept in 1% acidic methanol at 4 °C for 18 h to extract anthocyanins. Then, the extracts were subjected to a 5 min centrifugation at 12,000 rpm. After centrifugation, 50 μL of supernatant was separated and added into the extraction solution (150 μL). A microplate spectrophotomete was used to detect the absorbance of each sample at 530 nm (A_{530}) and 657 nm (A_{657}). The total anthocyanin content was calculated as (A_{530}–0.25 × A_{657}) g^{-1} fresh weight (FW).

As for the measurement of proanthocyanidins, the DMACA-HCl method described previously was utilized (Li et al., 1996). Shortly, about 0.15 g of samples ground in liquid nitrogen were incubated with 2 mL of 70% (V/V) aqueous acetone solution supplemented with 0.1% (W/V) L-ascorbic acid at 4 °C overnight. After centrifugation, the supernatant was mixed with 1.5 mL of diethyl ether in a new microcentrifuge tube and kept at −20 °C in the dark for separating into two phases. The 110 μL of lower phase was added into 55 μL of methanol and 28 μL of 2% (w/v) DMACA reagent. After 20 min incubation at room temperature, the proanthocyanidins were quantified by detecting the absorbance at 640 nm and indicated as A_{640} g^{-1} fresh weight (FW).

2.9. Histochemical assays

Arabidopsis seeds of wild type, *ttg1-1* mutant and homozygous transgenic plants were stained with 0.3% (w/v) DMACA dissolved in the methanol: 12 N HCl (1: 1, v/v) solutions (Pang et al., 2009). The seeds were incubated at room temperature for about 1 h before being rinsed with 70% (v/v) ethanol for several times. The phenotypes were visualized under a dissecting microscope.

3. Results

3.1. Isolation and sequence analysis of the putative WD40 protein from Freesia hybrida

The *Freesia* transcriptomic database assembled by transcripts from flowers at different developmental stages and five floral tissues aforementioned was used to isolate the candidate *TTG1* gene by *in situ* TBLASTN search (Li et al., 2016, 2017, 2019; Sun et al., 2015, 2016). Consequently, an unigene encoding potential WD40 protein was isolated and tentatively designated as *FhTTG1* which had an open reading frame of 1032 bp encoding a polypeptide of 343 amino acids (Table S2). The deduced FhTTG1 amino acid sequence had a 40 amino acid tandem repeat characterized by Gly-His (GH) and Trp-Asp (WD) doublet residues which were shared with other TTG1 orthologs available in the GenBank database (Fig. 1a). Moreover, the two amino acid residues (WD, FD, LD and WE) at the end of each WD-repeat motif were also highly conserved among the WD40 proteins involved in anthocyanin or proanthocyanidin biosynthesis in different species (Brueggemann et al., 2010; Liu et al., 2013; Pang et al., 2009; Taheri et al., 2012; Zohar et al., 2011).

To better define FhTTG1, a phylogenetic analysis of the known anthocyanin or proanthocyanidin biosynthesis related WD40 proteins was performed. Results showed that FhTTG1 fell within the well-supported monocot clade including WD40 proteins from *Zea mays* and *Oryza sativa*, suggesting a closer relationship with homologs from monocot species (Fig. 1b).

Additionally, the genomic structure of *FhTTG1* was also investigated by specific primers (Table S1) using genomic DNA of Red River® as template. Consequently, that the PCR products amplified from either cDNA or genomic DNA shared nearly the same length (Fig. S2). The PCR products were further sequenced and results turned out that the coding region of FhTTG1 was not interrupted by any introns which was consistent with other *TTG1* homologs identified (Fig. S3; Pang et al., 2009; Zohar et al., 2011; Taheri et al., 2012).

3.2. FhTTG1 showed a close correlation with anthocyanin and proanthocyanidin accumulations

To investigate whether the expression of *FhTTG1* was paralled with the accumulation of anthocyanin and/or proanthocyanidin in Red River®, the deposition of anthocyanin and proanthocyanidin, as well as the expression levels of *FhTTG1* were evaluated in 3 vegetative tissues, 5 flower developmental stages and 5 floral tissues (Fig. 2a and b). As results, the anthocyanin biosynthesis was initiated from non-pigmented flower buds (Stage 1), increased gradually and peaked in the fully opened flowers (Stage 5), while the proanthocyanidin was accumulated at a relatively stable state (Fig. 2c and d), which was in agreement with our previous work (Li et al., 2016). As for different tissues, the anthocyanin was dominantly accumulated in floral tissues, while proanthocyanidin was highly synthesized in toruses (Fig. 2e and f). Comparatively, the expression patterns of FhTTG1 coincided well with the anthocyanin accumulation during flower development (Fig. 3a). Moreover, FhTTG1 was mainly expressed in petals and toruses, which were the primary tissues that accumulated anthocyanins and proanthocyanidins, respectively (Fig. 3b). To further exploit the potential target genes regulated by FhTTG1, the expression profiles of *FhDFR3*, *FhLDOX1* and *Fh3GT1* were also investigated by qRT-PCR in aforementioned tissues and developmental stages. Generally, their expression levels increased and reached the highest expression level at stage 5 (Fig. 3a). Transcript analysis in different tissues revealed that significantly higher expression levels were mainly observed in petals, calyxes and toruses in which the anthocyanin or proanthocyanidin extremely accumulated (Fig. 3b). The similar expression patterns of *FhTTG1* and the structural genes suggested a potential regulation relationship between them. Taken together, the synchronous correlations between gene expressions and metabolite accumulations indicated that *FhTTG1* might play important roles in both anthocyanin and proanthocyanidin biosynthesis in *Freesia*.

3.3. FhTTG1 could complement the Arabidopsis ttg1 mutant

In order to further decipher the function of *FhTTG1* in anthocyanin or proanthocyanidin biosynthesis, the ectopic expression of *FhTTG1* in *Arabidopsis* was carried out to confirm its roles *in vivo*. The *Arabidopsis ttg1-1* mutant expressed a non-functional AtTTG1 protein because of the newly introduced termination codon by single C-to-T base transition, which resulted in the incapability of synthesizing anthocyanins in cotyledons or hypocotyls, and failed to accumulate brown tannins in seed coats, accompanied by the glabrous vegetative organs (Walker et al., 1999). Afterwards, the FhTTG1 transformants revealed that the seedlings restored anthocyanin accumulation in the cotyledons and hypocotyls, and the trichomes on leaves recovered as wild type (Fig. 4a). To examine whether the complementation of the seed coats was resulted from the synthesis of tannins, the seeds were stained by 4-dimethylaminocinnamaldehyde (DMACA) overnight and observed under a dissecting microscope. DMACA staining results suggested increased proanthocyanidin content in mature transgenic seeds compared with *ttg1-1* mutant (Fig. 4a). The transgenic lines were further confirmed for the expression of exogenous genes through RT-PCR, which indicated that the recovered phenotype might result from the expression of exogenous *FhTTG1* (Fig. 4b). Moreover, 1-week-old T3 seedlings cultured on 1/2 MS medium containing 3% w/v sucrose were sampled to determine the contents of total anthocyanins and proanthocyanidins. Consequently, transformants of *ttg1-1* mutant with *FhTTG1* resulted in the partial recovery of both anthocyanins and proanthocyanidins (Fig. 4c). With the purpose of targeting the candidate genes controlled by FhTTG1 in transgenic plants, the expression levels of genes participating in the flavonoid biosynthesis and trichome formation were further measured by qRT-PCR. Compared with *ttg1-1* mutant, both endogenous flavonoid biosynthesis related structural genes, e.g. *AtCHS*, *AtF3H*, *AtDFR*, *AtLDOX*, *At3GT and AtBAN*, and trichome formation related regulatory gene, *AtGL2*, were coordinately up-regulated (Fig. 4d). Herein, FhTTG1 might be postulated to perform versatile roles in multiple traits, including anthocyanin and proanthocyanidin biosynthesis and trichome formation, which resembled AtTTG1 in *Arabidopsis*.

3.4. The FhTTG1 transportation to the nucleus depended on the interactions with bHLH factors

Generally, WD40 proteins were not considered having any catalytic activity, but rather seemed to be a docking platform through interacting with several proteins simultaneously (Nocker and Ludwig, 2003). Many studies declared that WD40 proteins could only activate gene expressions in the presence of other components of MBW complex, such as bHLH proteins. To assess the involvement of FhTTG1 in potential MBW complexes in *Freesia*, GAL4-based transient *Arabidopsis* protoplast assays were employed to detect the potential interactions between FhTTG1 and FhbHLH factors. In this system, GD tag could identify and combine to the *GAL4* sequence when co-transfected with GAL4: GUS reporter plasmid. If FhTTG1 was a transactivator, it would be dragged to the *GAL4* sequence and close enough to activate *GUS* expression. As

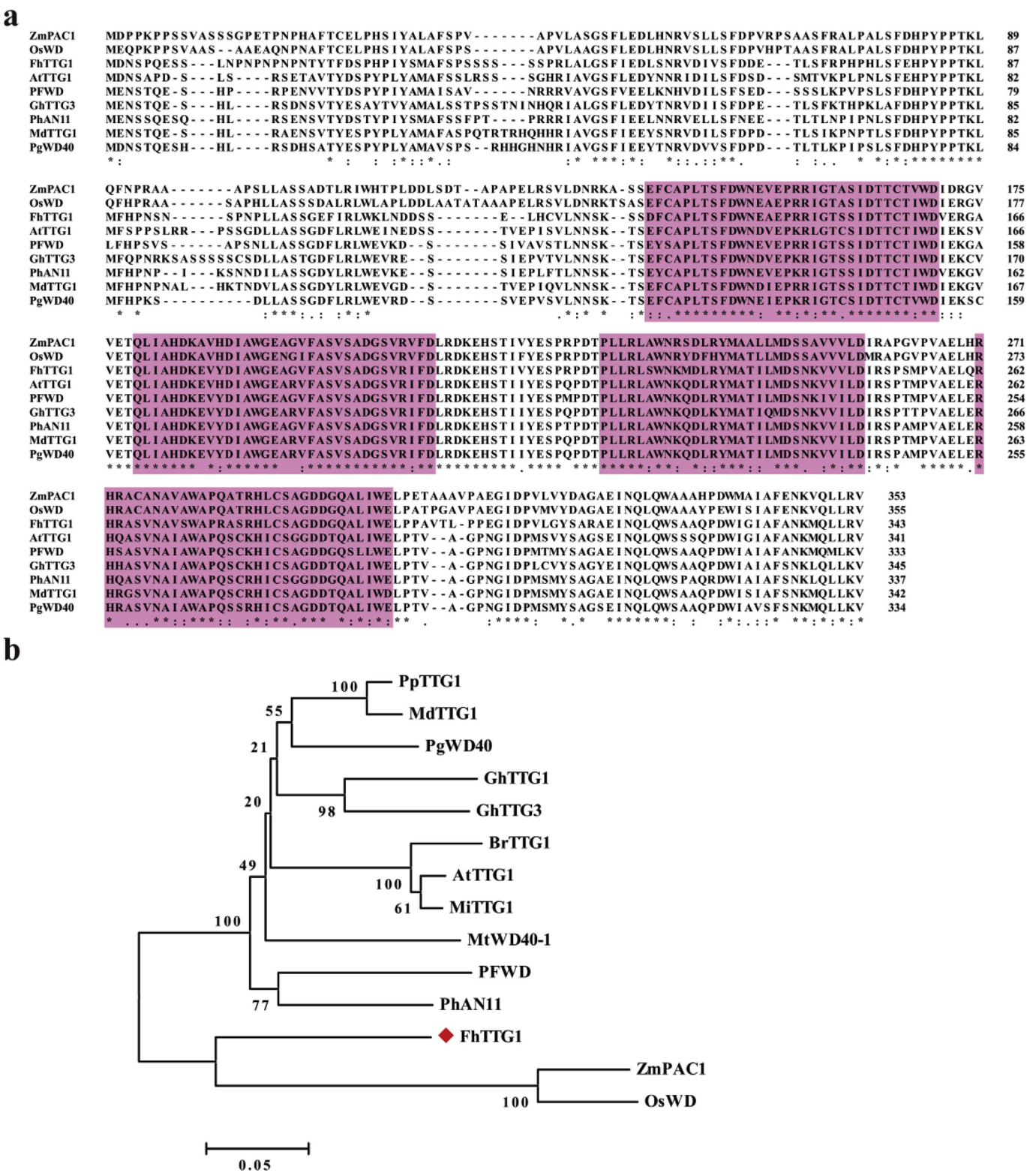

Fig. 1. Phylogenetic analysis of FhTTG1. (a) Sequence alignment of FhTTG1 and its closest homologs in the regulation of flavonoid biosynthesis. Numbers indicated the position of the last amino acid in each line of the proteins within the corresponding full-length protein sequence. *, identical amino acids;: or., similar amino acids. The WD40 repeat domains were indicated with purple boxes. (b) Phylogenetic relationships of selected WD40 proteins. Phylogenetic tree was constructed using the neighbor-joining method by the MEGA6 software. The reliability of the trees was tested using a bootstrapping method with 1000 replicates. Numbers indicated bootstrap values for 1000 replicates. FhTTG1 was indicated with red square. The GenBank accession numbers of the WD40 protein sequences were listed as follows: *Prunus persica* PpTTG1 (ACQ65867), *Malus domestica* MdTTG1 (GU173813), *Punica granatum* PgWD40 (HQ199314), *Gossypium hirsutum* GhTTG1 (AAM95641), GhTTG3 (AAM95645), *Perilla frutescens* PFWD (BAB58883), *Petunia hybrida* PhAN 11 (AAC18914), *Brassica rapa* BrTTG1 (ABQ10570), *Arabidopsis thaliana* AtTTG1 (Q9XGN1), *Matthiola incana* MiTTG1 (CAE53274), *Medicago truncatula* MtWD40-1 (ABW08112), *Zea mays* ZmPAC1 (AAM76742), *Oryza sativa* OsWD (BAF09665). . (For interpretation of the references to color in this figure legend, the reader is referred to the Web version of this article.)

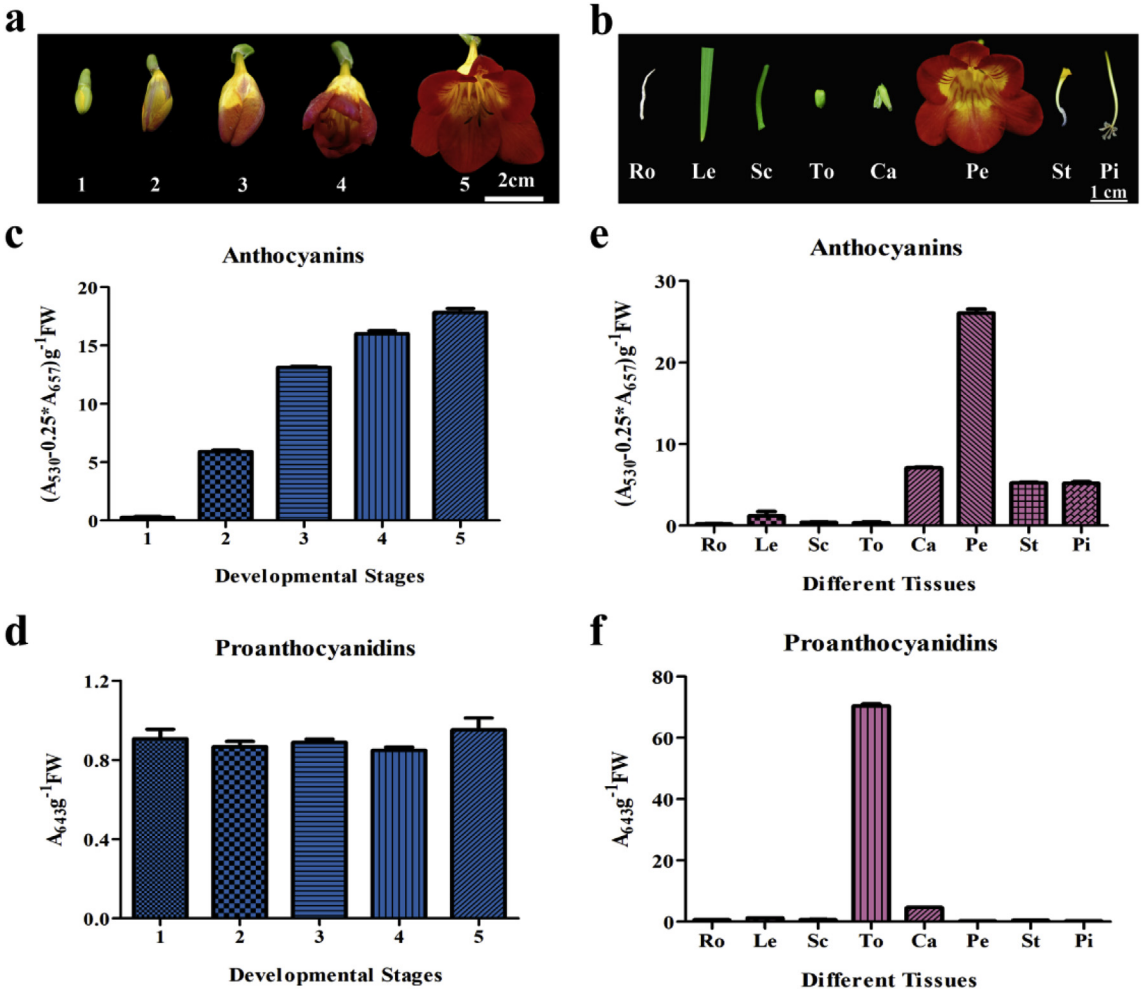

Fig. 2. Anthocyanin and proanthocyanidin accumulations in *Freesia hybrida*. (a) and (b) Five developmental stages of *Freesia* flowers and eight different tissues. 1–5, represented the flowers of different developmental stages. Ro, roots; Le, leaves; Sc, scapes; To, toruses; Ca, calyxes; Pe, petals; St, stamens; Pi, pistils. (c) and (d) Anthocyanin and proanthocyanidin accumulations at different developmental stages. (e) and (f) Anthocyanin and proanthocyanidin accumulations in different tissues. Data represented means ± SD of three biological replicates.

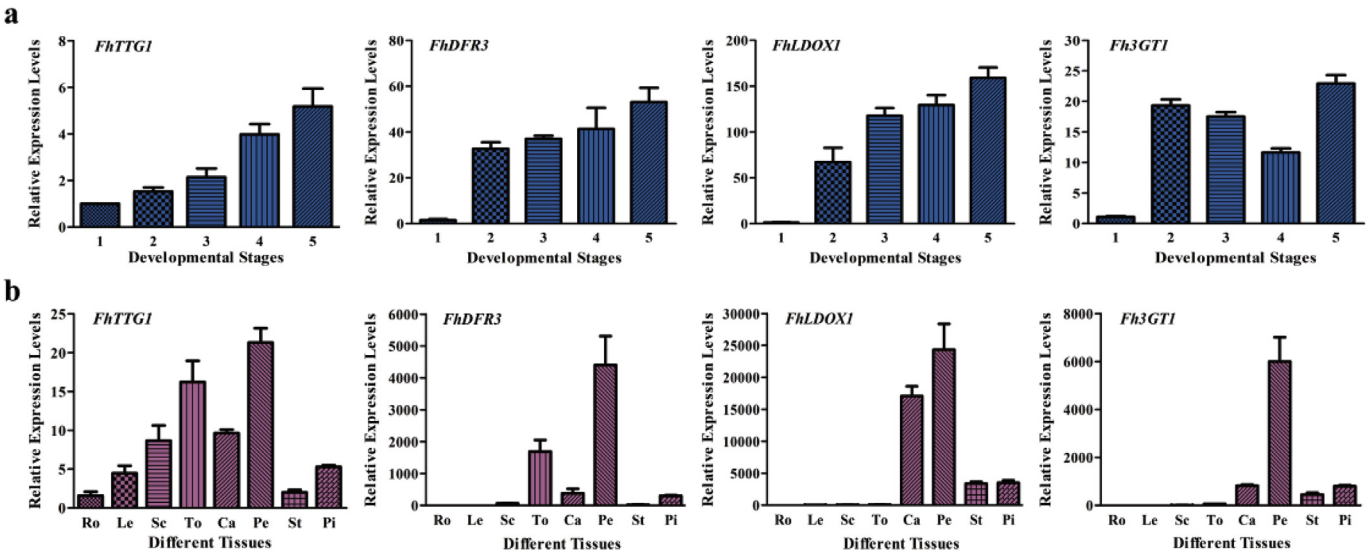

Fig. 3. Expression profiles of *FhTTG1, FhDFR3, FhLDOX1* and *Fh3GT1* in *Freesia hybrida*. (a) Expression levels of *FhTTG1*, *FhDFR3, FhLDOX1* and *Fh3GT1* in flowers at different developmental stages. (b) Expression levels of *FhTTG1*, *FhDFR3, FhLDOX1* and *Fh3GT1* in different tissues. 1–5, represented the flowers of different developmental stages. Ro, roots; Le, leaves; Sc, scapes; To, toruses; Ca, calyxes; Pe, petals; St, stamens; Pi, pistils. Data represented means ± SD of three biological replicates.

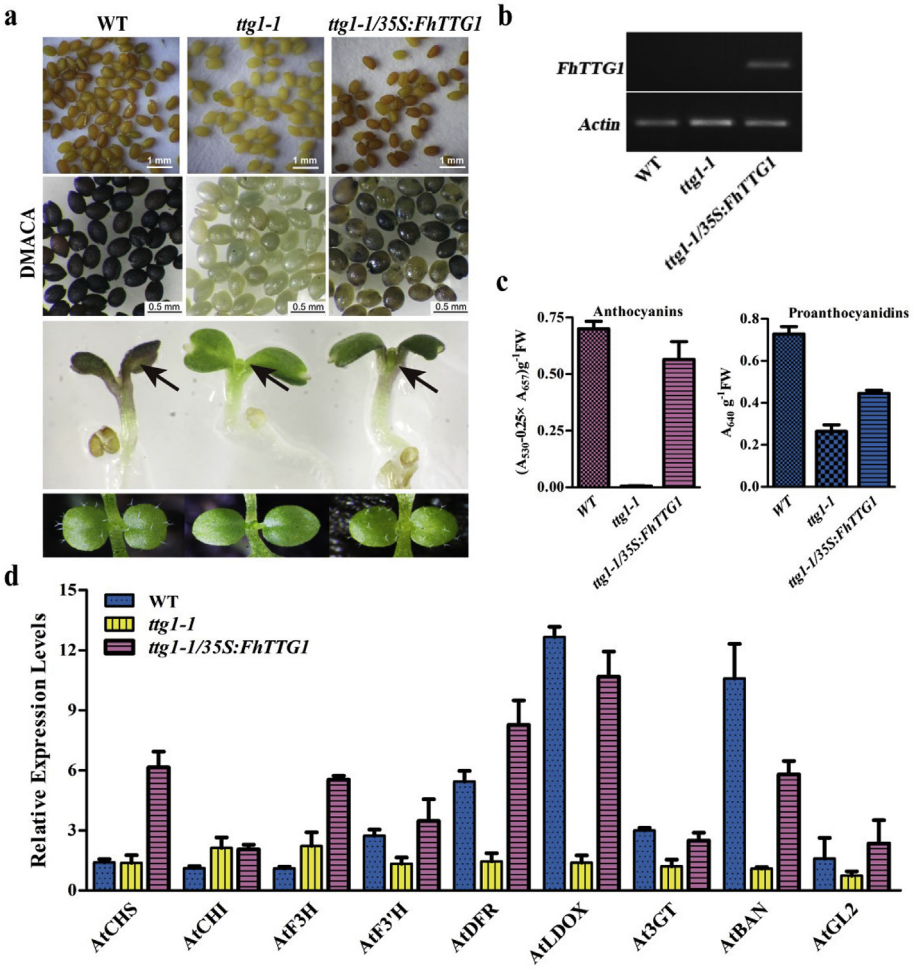

Fig. 4. Complementation analysis of FhTTG1 in *Arabidopsis ttg1-1* mutant. (a) Phenotypes of wild type (Ler-0), *ttg1-1* mutant and transgenic *Arabidopsis*. (b) Expression analysis of *FhTTG1* by RT-PCR in the wild type, *ttg1-1* mutant and *FhTTG1* transgenic lines. (c) Contents of anthocyanidins and proanthocyanidins in *Arabidopsis* seedlings. (d) Expression analysis of genes involved in anthocyanin and proanthocyanidin biosynthesis and trichome formation in *Arabidopsis* seedlings. Data represented the mean ± SD of three replicates.

results, GD-fused FhTTG1 presented an extremely weak GUS activity almost identical to the negative control, illustrating that FhTTG1 protein lacked transactivation capacity. However, FhTTG1 acquired high transactivation capacity when one or two copies of a strong activation domain VP16 were fused (Fig. 5a). The incapability of FhTTG1 in activating *GUS* expression in GAL4: GUS system promoted us to detect its repression activity in LexA-GAL4: GUS system. In this system, LD-VP16 was co-transfected with GD-FhTTG1 as effectors. The strong activation domain VP16 would be able to activate GUS expression when LD bond to LexA sequence. However, GD tagged FhTTG1 would intervene the activation of *GUS* if FhTTG1 was a repressor. Virtually, FhTTG1 actually presented an inhibition capacity when tested by the system (Fig. S4). Moreover, the GAL4-base system could also be used in detecting protein interactions. As reported in our earlier studies, GD tagged FhTT8L or FhGL3L showed little transactivation capacity (Li et al., 2016, 2019). If FhTTG1 could interact with either FhTT8L or FhGL3L, the FhTTG1-VP16 would be recruited to the promoter of *GUS* reporter gene and then activating *GUS* expression. Afterwards, the results indicated that FhTTG1 could interact with either FhTT8L or FhGL3L (Fig. 5b). BiFC assays were performed to additionally investigate the interactions between FhTTG1 and FhbHLH proteins in protoplasts isolated from *Freesia* calluses. NLS (nuclear localization signal)-RFP, a chemiric fluorescent protein (RFP) construct containing a nuclear localization signal, was also included in each transfection assay to mark the nucleus of transformed cells, including those in which no BiFC occurred, different combinations of transgenes encoding fusions of FhGL3L or FhTT8L to the N-terminal half of GFP (GFPN) and fusion of FhTTG1 to the C-terminal half of GFP (GFPC). As shown in Fig. 5c, the split GFP could be complemented in nucleus when FhTTG1 was co-transformed with FhbHLHs, indicating that FhTTG1 could interact with FhTT8L or FhGL3L and might function as a member of MBW complex. The same results could also be concluded by combinations of FhGL3L or FhTT8L to the C-terminal half of GFP (GFPC) and fusion of FhTTG1 to the N-terminal half of GFP (GFPN) in BiFC assays (Fig. S5).

To further study the significance of FhTTG1-FhbHLHs interaction observed in protoplasts, we then analyzed the intracellular localization of the single proteins by transfecting *Freesia* protoplasts with *35S*-driven transgenes encoding GFP fusions. As results, FhTTG1 showed a diffuse cellular distribution as GFP alone did in *Freesia* protoplasts (Fig. 6). It might be resulted from the absence of NLS or any other signal peptide in FhTTG1 (http://www.cbs.dtu.dk/services/SignalP/). However, transcription factors should mobilize into nucleus to fulfill their regulatory actions, and how did FhTTG1 act it remained further investigation. In contrast, FhGL3L and FhTT8L fused with GFP could be entirely or partially localized to the nucleus (Fig. 6). The intracellular localizations of FhTTG1, FhTT8L and FhGL3L were also reconfirmed by fusing GFP to the N-terminus of each protein and then transiently expressed in *Arabidopsis* protoplasts (Fig. S6). Therefore, it is reasonable to deduce that the nuclear import of FhTTG1 might depend on other MBW components, e.g., bHLH proteins, because of their interactions. To confirm

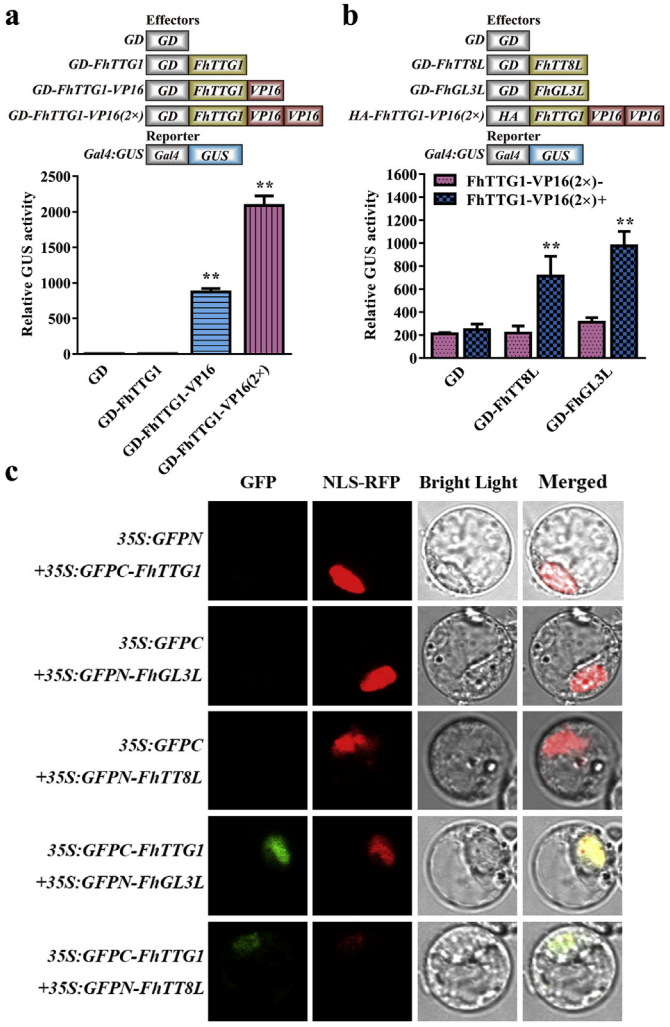

Fig. 5. FhTTG1 could interact with *Freesia* bHLH proteins. (a) Transactivation capacity analysis of FhTTG1 by GAL4: GUS system. (b) The interaction analysis between FhTTG1 and *Freesia* bHLH regulators based on GAL4: GUS system. The effector and reporter constructs were co-transfected as indicated in the diagram into *Arabidopsis* protoplasts. GUS activities were detected after protoplasts incubation for 21 h. Data represented the mean ± SD of three replicates. T-test was used to analyze the significant difference (*, $P < 0.05$; **, $P < 0.01$). (c) BiFC analysis of the interactions between FhTTG1 and FhbHLH regulators in *Freesia* protoplasts. Different construct combinations were transiently co-expressed in *Freesia* protoplasts. The fluorescence was observed under fluorescence microscope. NLS-RFP was the nuclear marker. The yellow fluorescence was merged by GFP and RFP. . (For interpretation of the references to color in this figure legend, the reader is referred to the Web version of this article.)

this idea, we performed the co-transfection assays with constructs expressing FhTTG1-GFP and FhTT8L or FhGL3L. In concert with our prospective, fluorescence of FhTTG1-GFP could be observed specially in nucleus when co-transfected with FhGL3L or FhTT8L, which implied that the nuclear import of FhTTG1 depended on *Freesia* bHLH proteins (Fig. 6).

3.5. *FhTTG1 could strengthen the expression of anthocyanin or proanthocyanidin related genes*

As noted in many species, MYB, bHLH, and WD40 proteins collaboratively activated the transcription of anthocyanin or proanthocyanidin biosynthetic genes (Hichri et al., 2011; Verweij et al., 2016). In *Freesia*, the MYB regulator FhMYB5 was recently characterized to

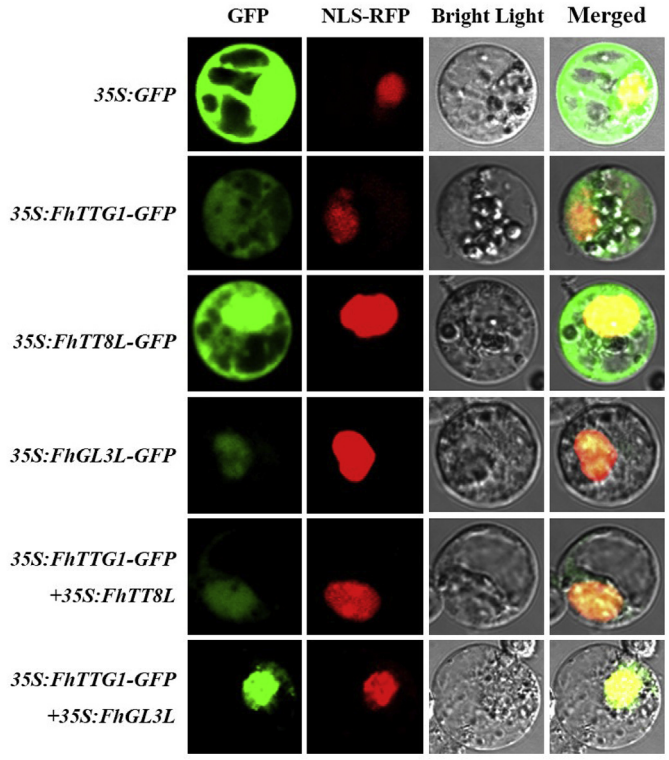

Fig. 6. Intracellular localizations of C-terminal fusion FhTTG1, FhTT8L and FhGL3L in *Freesia* Protoplast. Different combinations of constructs were transiently transfected into *Freesia* protoplasts and incubated for 21 h. GFP fluorescences were captured by laser scanning confocal microscope. NLS-RFP was used as the nuclear marker. The yellow fluorescence was merged by GFP and RFP. . (For interpretation of the references to color in this figure legend, the reader is referred to the Web version of this article.)

function in both anthocyanin and proanthocyanidin biosynthesis by interacting with bHLH factors FhTT8L and FhGL3L (Li et al., 2019). To further elucidate the roles of FhTTG1 in anthocyanin and proanthocyanidin biosynthesis, *FhMYB5*, *FhTT8L*, *FhGL3L* and *FhTTG*1 were either transfected alone or co-transfected into *Freesia* protoplasts with different combinations to check their capacities in activating *GUS* reporter gene promoted by *Freesia FhDFR3* promoter. Outstandingly, *FhDFR3* promoter could be highly activated when *FhMYB5* was co-transfected with *FhbHLH* regulators, which was also verified in our earlier study (Li et al., 2019). Additionally, the co-transfection of *FhTTG1* could significantly strengthen the MYB-bHLH effects on *FhDFR3* promoter (Fig. 7a). Moreover, another MYB regulator FhPAP1 was also isolated from *Freesia* and primarily characterized to promote anthocyanin accumulation by interacting with bHLH factors (data not published). Herein, the effects of FhTTG1 on anthocyanin biosynthetic genes were further consolidated by transiently expressing *FhPAP1*, *FhTTG1*, *FhTT8L* or *FhGL3L* in combination with *GUS* reporter constructs promoted by *Freesia FhLDOX1* or *Fh3GT1* promoters. Consequently, significant GUS activities were detected in protoplasts transfected simultaneously with *FhPAP1*, *FhTT8L* or *FhGL3L* and *FhTTG1*, consolidating that FhTTG1 could enhance the activation efficiency of the MYB-bHLH complex (Fig. 7b and c). Taken together, the MYB-bHLH-FhTTG1 triumvirate might be povital in both anthocyanin and proanthocyanidin biosynthesis of *Freesia hybrida*.

3.6. *FhTTG1 was functionally exchangeable with Arabidopsis TTG1 gene*

As an ortholog of AtTTG1, FhTTG1 was proved to function in either *Freesia* or *Arabidopsis*. However, whether FhTTG1 and AtTTG1 functioned in a conserved or divergent way was not fully investigated. To

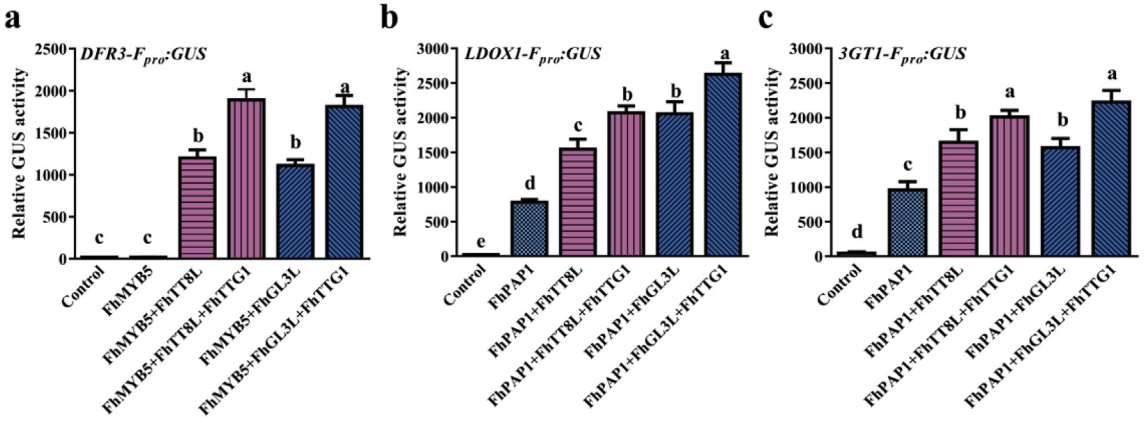

Fig. 7. FhTTG1 collaborated with FhbHLHs to regulate anthocyanin and proanthocyanidin biosynthesis related genes in *Freesia*. *Freesia* protoplasts were transfected with different combinations of effector constructs indicated in the bottom of each diagram to detect the GUS activities promoted by *Freesia FhDFR3* promoter (a), *FhLDOX1* promoter (b) and *Fh3GT1* promoter (c), respectively. Values were mean ± SD of three replicates. Statistical differences were calculated by one-way ANOVA (Ducan, $p < 0.05$).

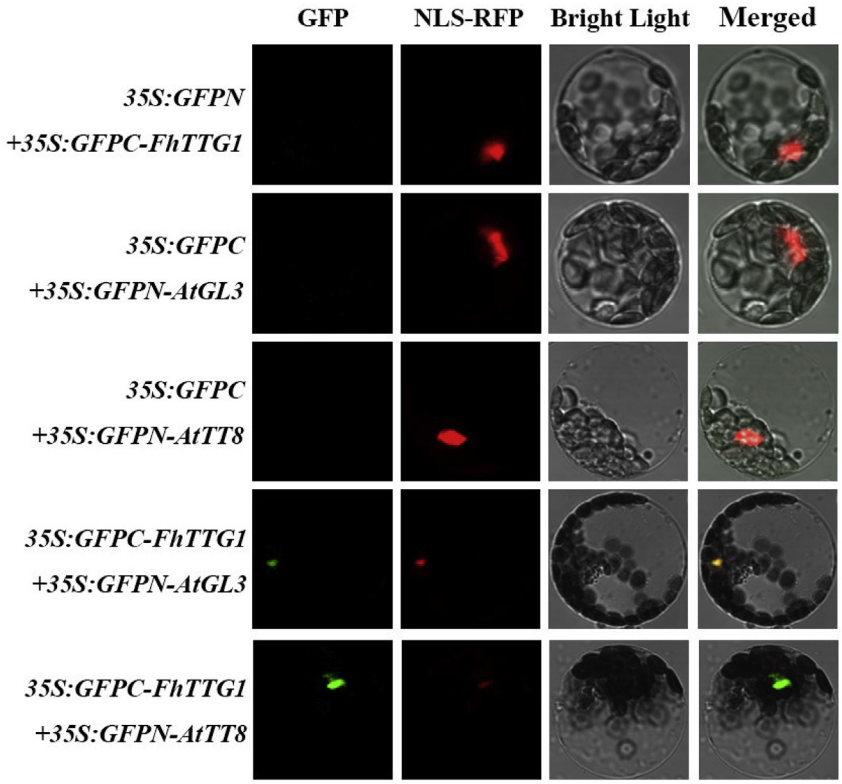

Fig. 8. FhTTG1 could interact with AtbHLHs in *Arabidopsis* protoplasts. Different combinations of constructs were transiently co-expressed in *Arabidopsis* protoplasts. BiFC fluorescence was observed under fluorescence microscope. NLS-RFP was the nuclear marker.

further investigate the precise mechanism of FhTTG1 in *Arabidopsis*, the BiFC assays were employed to detect the interactions between FhTTG1 and two endogenous IIIf bHLH transcription factors, AtTT8 and AtGL3, which involved in flavonoid biosynthesis and cell fate determination in *Arabidopsis*. Results showed that GFP fluorescence was only captured when *GFPC-TTG1* was co-expressed with *GFPN-AtTT8/AtGL3*, whereas no interaction was detectable when *GFPC-TTG1* was replaced by free *GFPC* or *GFPN-AtTT8/AtGL3* by free GFPN (Fig. 8). The results indicated that FhTTG1 and the homologous AtTTG1 were interchangeable regarding their capacity of interacting with AtTT8 or AtGL3. Moreover, the GAL4-based *Arabidopsis* protoplast transient transfection system was also carried out to test the interactions between FhTTG1 and AtTT8 or AtGL3. Results demonstrated that FhTTG1 could interact with either AtTT8 or AtGL3 to activate the *GUS* reporter gene (Fig. 9a), indicating that new ternary complexes AtMYB-AtTT8/AtGL3-FhTTG1 might be formed and functioned in transgenic plants. In *Arabidopsis*, AtTTG1 was usually considered to stabilize the interaction between AtMYB and AtbHLH, and this was further reinforced by the results that FhTTG1 could interact with bHLH proteins as mentioned above. To further certify the exchangeable function of FhTTG1 with AtTTG1, the ability of the newly formed MBW complexes containing FhTTG1 in the regulating of *AtDFR* and *AtBAN* was tested. Therefore, AtTT8 and AtGL3, and two MYB proteins, i.e. AtPAP1 and AtTT2, were combinatorially transfected with the *GUS* reporter constructs driven by the target promoters (*AtDFR and AtBAN*) at the presence or absence of FhTTG1. Consequently, stronger GUS activities were detected when

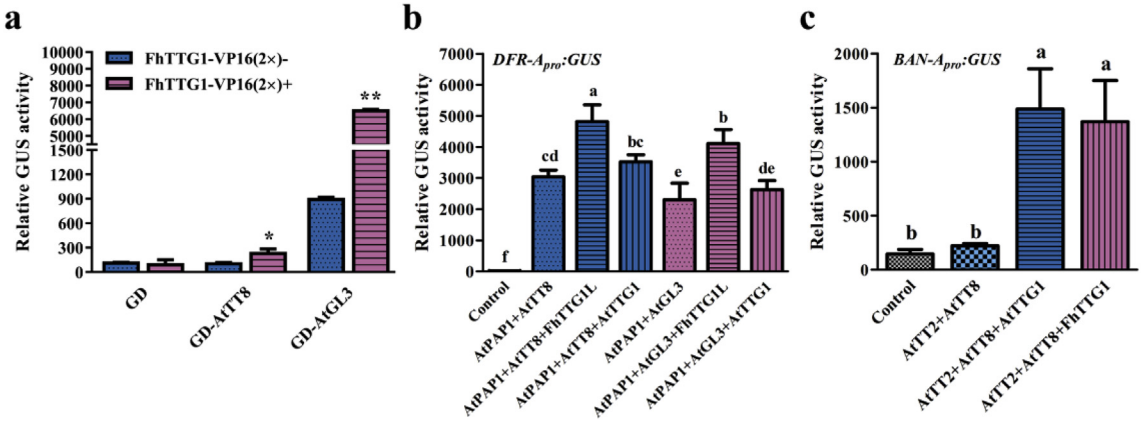

Fig. 9. FhTTG1 physically interacted with *Arabidopsis* bHLHs to activate *AtDFR* and *AtBAN*. (a) Interactions between FhTTG1 and *Arabidopsis* AtTT8 or AtGL3 detected by GAL4-based system. (b) and (c) *Arabidopsis* protoplasts were transfected with different combinations of effector constructs indicated in the bottom of each diagram to detect the GUS activities promoted by *Arabidopsis AtDFR* promoter (b) and *AtBAN* promoter (c), respectively. Values were mean ± SD of three replicates. One-way ANOVA was carried out to compare statistical differences (Ducan, $p < 0.05$).

WD40 proteins were co-expressed, emphasizing the fact that AtMYB-AtbHLH-FhTTG1, consistent with the AtMYB-AtbHLH-AtTTG1, could efficiently activate their target gene promoters (Fig. 9b and c). In addition, AtTT2 and AtTT8 could only significantly activate *AtBAN* at the presence of FhTTG1 or AtTTG1, implying a crucial role of WD40 protein in *Arabidopsis* proanthocyanidin biosynthesis (Fig. 9c).

4. Discussion

4.1. FhTTG1 was a functional homologue of Arabidopsis TTG1 gene

Presently, a sequence encoding putative WD-repeat protein was isolated by transcriptomic analysis with AtTTG1 as probe and subsequently named as FhTTG1. As for amino acid sequence, FhTTG1 shared 69% similarity with AtTTG1 (Table S2). In contrast to other regulators such as bHLH factors, WD40 proteins have higher degree of conservation among plant species. For example, only about 30% identity was observed between any two members of the following bHLH homologs: AtTT8, AtGL3 in *A. thaliana* (Nesi et al., 2000; Payne et al., 2000), B/R in *Z. mays* (Chandler et al., 1989; Ludwig et al., 1989), PhAN 1, PhJAF13 in *P. hybrida* (Quattrocchio et al., 1998; Spelt et al., 2000), and FhTT8L, FhGL3L in *F. hybrida* (Li et al., 2016). Further analysis revealed that four WD-repeat motifs and amino acid residues WD, FD, LD and WE that were highly conserved in anthocyanin biosynthesis related WD40 proteins in different species were also observed in FhTTG1 (Fig. 1a), implying the potential role of FhTTG1 in regulating anthocyanin biosynthesis. This was also reinforced by phylogenetic analysis as FhTTG1 from *Freesia* closely clustered with ZmPAC1 which was responsible for anthocyanin accumulation of scutellum and aleurone in maize seed and could complement *Arabidopsis ttg1-1* mutant to restore multiple phenotypes (Carey and Chandler, 2004). Furthermore, the expression of *FhTTG1* resembled well with anthocyanin and proanthocyanidin biosynthesis in plant tissues (Fig. 2). Additionally, the expression pattern of *FhTTG1* was similar with late structural genes, which showed high levels at stage 5 and in petals (Fig. 3). Actually, *FhTTG1* also expressed synergistically with other late anthocyanin biosynthetic genes, *FhDFR1/2* and *FhLDOX2*, both of which showed gradually increasing expression patterns in the flower development process (Li et al., 2017). When introduced into *Arabidopsis ttg1-1* mutant plants, FhTTG1 could obviously increase the flavonoid accumulation by strengthening the endogenous anthocyanin biosynthesis related genes including *AtDFR*, *AtLDOX*, *At3GT*, as well as specific proanthocyanidin biosynthetic gene *AtBAN*, which consequently complemented the pigmentation loss in seed coats as well as cotyledons and hypocotyls (Fig. 4). Meanwhile, the trichome formation related *AtGL2* was also dramatically activated which subsequently initiated the leaf trichome formation. Taken together, it can be concluded that the newly identified FhTTG1 could function in both anthocyanin and proanthocyanidin biosynthesis and cell fate determination.

4.2. The protein interactions were critical in regulatory mechanisms

Generally, transcription factors with NLS will be imported into the nucleus to exert their regulatory actions. Meanwhile, transcription factors without NLSs could also be transported into nucleus in the aid of proteins with NLSs. Subcellular localization predictions implied that FhGL3L had a NLS and might localize into nucleus whereas FhTTG1 had ambiguous intracellular localization signals (http://www.cbs.dtu.dk/services/SignalP/). The interaction of FhTTG1 with FhGL3L suggested that FhTTG1 might be transported into nucleus with the help of FhGL3L (Figs. 5 and 6). Furthermore, transient protoplast transfection assays revealed that the FhTTG1-GFP fusion protein could localize in nucleus or cytoplasm in the presence or absence of FhbHLH proteins (Fig. 6). There was a similar case for PFWD which was observed in cytoplasm when solitarily expressed. However, PFWD could be translocated to the nucleus when co-expressed with MYC-RP in onion cells (Sompornpailin et al., 2002). In addition, grapevine VvMYC1 was supposed to help delivering other binding partners such as WD40 or another partner in the cytoplasm to the nucleus and then regulate the flavonoid pathway (Hichri et al., 2010). All the results above emphasized the bHLH-WD40 interaction was of crucial importance for WD40. However, unlike the other bHLH proteins, FhTT8L-GFP had a diffuse distribution when expressed alone in protoplasts (Fig. 6). In addition, the co-expression of FhTT8L and FhTTG1 prompted FhTTG1 to be imported into nucleus, which may be resulted from that the interaction might change protein conformations and thus the new NLS would be exposed. And the results herein also implied functional divergences of FhbHLHs during evolution which was indicated in our earlier study (Li et al., 2016). Interestingly, FhTTG1 could also interact with AtTT8 and AtGL3 (Figs. 8 and 9a), indicating that FhTTG1 and AtTTG1 were interchangeable and that FhTTG1-AtbHLHs interactions were also critical in regulatory mechanisms in transgenic plants.

4.3. FhTTG1 functioned as a constituent of MBW complex in regulating multiple physiological traits

As mentioned above, the most common and defining structural feature of WDR proteins was the tandem WD-repeat motif sequence which adopted bladed β-propeller-like structures containing potential surfaces indispensable for molecular interactions (Miller et al., 2015).

Virtually, this was also validated in FhTTG1 which was further found to interact with AtbHLHs and FhbHLHs aforementioned.

Till now, more and more MBW complexes involved in various physiological processes have been characterized and the most in-depth studies were elucidated in *Arabidopsis thaliana*. The triumvirate has been proved to be implicated in numerous events, such as anthocyanin and proanthocyanidin biosynthesis, trichome formation, root hair patterning and seed coat mucilage production (Lepiniec et al., 2006). In many species, distinct MBW complexes share the same WDR constituents. For example, in *Arabidopsis*, AtTTG1 was enrolled in MBW complexes AtPAP1/2/3-AtEGL3/GL3/TT8-AtTTG1 which dominated the regulation of anthocyanin biosynthesis, and AtMYB5/TT2-AtGL3/EGL3/TT8-AtTTG1 which activated the proanthocyanidin biosynthetic genes. Moreover, AtGL1-AtGL3/EGL3-AtTTG1 was required by trichome formation. In monocot maize, MBW complexes, ZmC1/PL1-ZmR/B-ZmPAC1, were found to control the anthocyanin biosynthesis. Actually in MBW complexes, the bHLHs from subgroup IIIf were supposed to arise about 400 million years ago, early before the origin of the mosses (Carreteropaulet et al., 2010; Pires and Dolan, 2010). Comparatively, TTG1 sequences only emerged in angiosperms rather than gymnosperms or more ancient plant lineages (Brueggemann et al., 2010; Humphries et al., 2005; Zohar et al., 2011). Consequently, WDR-containing protein was considered as a new member recruited by bHLH dimmers to aid in complex stability during plant evolution (Zhao et al., 2008).

The activation of anthocyanin or proanthocyanidin biosynthesis by MBW complexes might be a more ancient process compared with the regulation of trichome formation in evolution. Because of the regulation of trichome fate by MBW triumvirates was only found in some Rosid species (*Arabidopsis*) and not in dicot species belonging to the Asterids or in monocots (Serna and Martin, 2006; Verweij et al., 2016). However, the newly formed MBW complexes containing FhTTG1 in *Arabidopsis* could regulate both anthocyanin and proanthocyanidin biosynthesis and trichome formation, indicating the conservation and pleiotropy of *TTG1* gene.

To date, more and more evidences have verified that WD40 protein did not seem to be dispensable. In *M. truncatula,* because of the loss of function of MtWD40-1, the levels of aurone and isoflavone glycosides were found to be reduced in roots as well as benzoic acids, which could be hardly detected in seeds (Pang et al., 2009). Furthermore, as the phenotype showed in *Arabidopsis ttg1-1* mutant, several physiological developments were severely affected, such as deficiency in seed coat mucilage, flavonoid accumulation and trichomes. Further investigations on gene expression levels also confirmed the indispensable roles of TTG1 in regulating anthocyanin and proanthocyanidin biosynthesis. Analysis in transient protoplast transfection assays against promoters of *DFR*, *BAN* and *UFGT* consolidated that the presence of FhTTG1 or AtTTG1 was of great concern (Figs. 7 and 9). Similar result was found previously that the activation efficacy of *BAN* promoter was almost four times higher in *Arabidopsis* protoplasts co-transfected with *AtTT2*, *AtTT8* and *AtTTG1* in contrast to the combination without *AtTTG1* (Baudry et al., 2004). In addition, loss function of *AtTTG1* seemly had no significant effect on the early anthocyanin biosynthetic genes, which was consistent with the widely accepted regulatory model that MBW complex was mainly responsible for the activations of late biosynthetic genes in *Arabidopsis*, e.g. *AtDFR*, *AtLDOX* and *At3GT* (Jaakola, 2013; Xu et al., 2015). In contrast, the overexpression of *FhTTG1* markedly up-regulated several early genes, e.g. *AtCHS* and *AtF3H*, except the highly expressed late biosynthetic genes (Fig. 4d). The up-regulation of *AtCHS* and *AtF3H* could be partly resulted from the enriched metabolic flux in FhTTG1 transformants. Alternatively, *AtCHS* and *AtF3H* might be potential target genes of FhTTG1 considering recent findings of Zhu et al. (2015), who declared that the corresponding MBW complexes from either *Arabidopsis* or *Ipomoea purpurea* could positively regulate almost all the anthocyanin biosynthetic genes. In conclusion, the results herein demonstrated that WD40 was probably helpful but not necessary in regulating early anthocyanin biosynthetic genes, which was also validated by earlier studies (Morita et al., 2006; Xu et al., 2014).

Interestingly, there are still several possible limitations in this work. For example, FhTTG1 was proved to promote anthocyanin and proanthocyanidin accumulations and trichome formation, it encoded a protein with transcriptional repression capacity detected by transient assays, however (Fig. S4). This might be partly accounted by the versatile roles of WD40 as AtTTG1 can reduce the levels of seed storage proteins by negatively regulate *Arabidopsis 2S3* gene which encodes a 2 S albumin precursor (Chen et al., 2015). Additionally, FhTTG1 was proved to complement the glabrous phenotype in *Arabidopsis*, there are no trichomes in *Freesia* flowers or leaves, however. What are the precise roles of FhTTG1 in *Freesia* and how the WD40 proteins function in a conserved or divergent way after the separation of monocots and dicots are not fully investigated. Steady efforts towards deciphering all possible functions of FhTTG1 in *Freesia* might contribute to decipher the precise mechanisms of FhTTG1 in other biological processes.

5. Conclusions

In this study, we identified a functional homologue of *Arabidopsis TTG1* gene, designated as *FhTTG1*, in *F. hybrida*. It showed positive correlations with anthocyanin and proanthocyanidin accumulations in *Freesia* flowers. Furthermore, FhTTG1 could interact with FhTT8L or FhGL3L and might function as a member of *Freesia* MBW complex to control the anthocyanin and proanthocyanidin biosynthesis *in vivo*. In addition, FhTTG1 could complement the *Arabidopsis ttg1-1* mutant by interacting with AtbHLHs to stabilize the MYB-bHLH complex in regulating multiple physiological processes such as anthocyanin and proanthocyanidin biosynthesis and trichome formation. The results indicated that FhTTG1 and AtTTG1 were interchangeable in these respects. However, the precise regulatory mechanism of FhTTG1 still needs to be further investigated in *Freesia per se* considering its potential versatile roles. The present study will not only contribute to the establishment of the regulatory mechanism in anthocyanin or proanthocyanidin biosynthesis in *Freesia* but also provide new evolutionary insights of the WD40 proteins from monocot plants and dicot plants.

Contributions

XS, YL, SY, RG and LZ performed most of the experiments. TB, TH helped in seedling planting and sample preparation, SW helped analyze the results, XG designed the experiments and wrote the manuscript together with XS and YL. LW helped design the experiments. All authors read and approved the final manuscript.

Acknowledgements

This work was supported by the National Natural Science Foundation of China [grant number 31570295, 31300271], the China Postdoctoral Science Foundation funded project [grant number 2018M641761], the Department of Science and Technology of Jilin Province [grant number 20190201299JC, 20190303095SF], the Program for Introducing Talents to Universities [grant number B07017] and the Fundamental Research Fund for the Central Universities [grant number 2412017FZ019]. The funders had no role in study design, data collection and analysis, decision to publish, or preparation of the manuscript.

Appendix A. Supplementary data

Supplementary data to this article can be found online at https://doi.org/10.1016/j.plaphy.2019.05.015.

References

An, X.H., Tian, Y., Chen, K.Q., Wang, X.F., Hao, Y.J., 2012. The apple WD40 protein MdTTG1 interacts with bHLH but not MYB proteins to regulate anthocyanin accumulation. J. Plant Physiol. 169 (7), 710–717.

Baudry, A., Heim, M.A., Dubreucq, B., Caboche, M., Weisshaar, B., Lepiniec, L., 2004. TT2, TT8, and TTG1 synergistically specify the expression of BANYULS and proanthocyanidin biosynthesis in *Arabidopsis thaliana*. Plant J. 39 (3), 366–380.

Bent, A., 2006. *Arabidopsis thaliana* floral dip transformation method. Methods Mol. Biol. 343, 87–103.

Brueggemann, J., Weisshaar, B., Sagasser, M., 2010. A WD40-repeat gene from *Malus* x *domestica* is a functional homologue of *Arabidopsis thaliana TRANSPARENT TESTA GLABRA1*. Plant Cell Rep. 29 (3), 285–294.

Carey, C.C., Strahle, J.T., Selinger, D.A., Chandler, V.L., 2004. Mutations in the pale aleurone color 1 regulatory gene of the *Zea mays* anthocyanin pathway have distinct phenotypes relative to the functionally similar *TRANSPARENT TESTA GLABRA1* gene in *Arabidopsis thaliana*. Plant Cell 16 (2), 450–464.

Carreteropaulet, L., Galstyan, A., Roigvillanova, I., Martínezgarcía, J.F., Bilbaocastro, J.R., Robertson, D.L., 2010. Genome-wide classification and evolutionary analysis of the bHLH family of transcription factors in Arabidopsis, poplar, rice, moss, and algae. Plant Physiol. 153 (3), 1398–1412.

Chandler, V.L., Radicella, J.P., Robbins, T.P., Chen, J., Turks, D., 1989. Two regulatory genes of the maize anthocyanin pathway are homologous: isolation of *B* utilizing *R* genomic sequences. Plant Cell 1 (12), 1175–1183.

Chen, M., Zhang, B., Li, C., Kulaveerasingam, H., Chew, F.T., Yu, H., 2015. *TRANSPARENT TESTA GLABRA1* regulates the accumulation of seed storage reserves in *Arabidopsis*. Plant Physiol. 169 (1), 391–402.

Davies, K.M., Albert, N.W., Schwinn, K.E., 2012. From landing lights to mimicry: the molecular regulation of flower colouration and mechanisms for pigmentation patterning. Funct. Plant Biol. 39 (8), 619–638.

De, V.N., Quattrocchio, F., Mol, J., Koes, R., 1997. The an11 locus controlling flower pigmentation in petunia encodes a novel WD-repeat protein conserved in yeast, plants, and animals. Genes Dev. 11 (11), 1422–1434.

Gao, F., Liu, B., Li, M., et al., 2018. Identification and characterization of terpene synthase genes accounting for volatile terpene emissions in flowers of *Freesia x hybrida*. J. Exp. Bot. 69 (18), 4249–4265.

Gonzalez, A., Mendenhall, J., Huo, Y., Lloyd, A., 2009. TTG1 complex MYBs, MYB5 and TT2, control outer seed coat differentiation. Dev. Biol. 325 (2), 412–421.

Hichri, I., Heppel, S.C., Pillet, J., et al., 2010. The basic helix-loop-helix transcription factor MYC1 is involved in the regulation of the flavonoid biosynthesis pathway in grapevine. Mol. Plant 3 (3), 509–523.

Hichri, I., Barrieu, F., Bogs, J., Kappel, C., Delrot, S., Lauvergeat, V., 2011. Recent advances in the transcriptional regulation of the flavonoid biosynthetic pathway. J. Exp. Bot. 62 (8), 2465–2483.

Humphries, J.A., Walker, A.R., Timmis, J.N., Orford, S.J., 2005. Two WD-repeat genes from cotton are functional homologues of the *Arabidopsis* thaliana *TRANSPARENT TESTA GLABRA1 (TTG1*) gene. Plant Mol. Biol. 57 (1), 67–81.

Jaakola, L., 2013. New insights into the regulation of anthocyanin biosynthesis in fruits. Trends Plant Sci. 18 (9), 477–483.

Ju, Z., Sun, W., Meng, X., et al., 2018. Isolation and functional characterization of two 5-*O*-glucosyltransferases related to anthocyanin biosynthesis from *Freesia hybrida*. Plant Cell Tiss Org 135 (1), 99–110.

Koes, R., Verweij, W., Quattrocchio, F., 2005. Flavonoids: a colorful model for the regulation and evolution of biochemical pathways. Trends Plant Sci. 10, 236–242.

Lepiniec, L., Debeaujon, I., Routaboul, J.M., et al., 2006. Genetics and biochemistry of seed flavonoids. Annu. Rev. Plant Biol. 57 (1), 405–430.

Li, Y.G., Tanner, G., Larkin, P., 1996. The DMACA-HCl protocol and the threshold proanthocyanidin content for bloat safety in forage legumes. J. Sci. Food Agric. 70 (1), 89–101.

Li, Y., Shan, X., Gao, R., et al., 2016. Two IIIf clade-bHLHs from *Freesia* hybrida play divergent roles in flavonoid biosynthesis and trichome formation when ectopically expressed in*Arabidopsis*. Sci. Rep. 6, 30514. https://doi.org/10.1038/srep30514.

Li, Y., Liu, X., Cai, X., et al., 2017. Dihydroflavonol 4-reductase genes from *Freesia* hybrida play important and partially overlapping roles in the biosynthesis of flavonoids. Front. Plant Sci. 8 (428). https://doi.org/10.3389/fpls.2017.00428.

Li, Y., Shan, X., Zhou, L., et al., 2019. The R2R3 MYB factor FhMYB5 from *Freesia hybrida* contributes to the regulation of anthocyanin and proanthocyanidin biosynthesis. Front. Plant Sci. 9, 1935. https://doi.org/10.3389/fpls.2018.01935.

Liu, X., Feng, C., Zhang, M., Yin, X., Xu, C., Chen, K., 2013. The *MrWD40-1* gene of Chinese bayberry (*Myrica rubra*) interacts with MYB and bHLH to enhance anthocyanin accumulation. Plant Mol. Biol. Rep. 31 (6), 1474–1484.

Livak, K.J., Schmittgen, T.D., 2001. Analysis of relative gene expression data using real-time quantitative PCR and the 2 -ΔΔCT method. Methods 25 (4), 402–408.

Ludwig, S.R., Habera, L.F., Dellaporta, S.L., Wessler, S.R., 1989. *Lc*, a member of the maize *R* gene family responsible for tissue-specific anthocyanin production, encodes a protein similar to transcriptional activators and contains the *myc*-homology region. P Natl Acad Sci USA 86 (18), 7092–7096.

Matus, J.T., Poupin, M.J., Cañón, P., Bordeu, E., Alcalde, J.A., Arcejohnson, P., 2010. Isolation of WDR and bHLH genes related to flavonoid synthesis in grapevine (*Vitis vinifera L.*). Plant Mol. Biol. 72 (6), 607–620.

Miller, J.C., Chezem, W.R., Clay, N.K., 2015. Ternary WD40 repeat-containing protein complexes: evolution, composition and roles in plant immunity. Front. Plant Sci. 6, 1108. https://doi.org/10.3389/fpls.2015.01108.

Morita, Y., Saitoh, M., Hoshino, A., Nitasaka, E., Iida, S., 2006. Isolation of cDNAs for R2R3-MYB, bHLH and WDR transcriptional regulators and identification of *c* and *ca* mutations conferring white flowers in the Japanese morning glory. Plant Cell Physiol. 47 (4), 457–470.

Murashige, T., Skoog, F., 1962. A revised medium for rapid growth and bioassays with tobacco tissue cultures. Physiol. Plantarum 15 (3), 473–497.

Naval, M.D.M., Gil-Muñoz, F., Lloret, A., et al., 2016. A WD40-repeat protein from persimmon interacts with the regulators of proanthocyanidin biosynthesis DkMYB2 and DkMYB4. Tree Genet. Genomes 12 (1), 1–11.

Nesi, N., Debeaujon, I., Jond, C., Pelletier, G., Caboche, M., Lepiniec, L., 2000. The *TT8* gene encodes a basic helix-loop-helix domain protein required for expression of *DFR* and *BAN* genes in *Arabidopsis* siliques. Plant Cell 12 (10), 1863–1878.

Nocker, S.V., Ludwig, P., 2003. The WD-repeat protein superfamily in *Arabidopsis*: conservation and divergence in structure and function. BMC Genomics 4, 50. https://doi.org/10.1186/1471-2164-4-50.

Pandey, A., Misra, P., Bhambhani, S., Bhatia, C., Trivedi, P.K., 2014. Expression of *Arabidopsis* MYB transcription factor, AtMYB111, in tobacco requires light to modulate flavonol content. Sci. Rep. 4 (5), 5018. https://doi.org/10.1038/srep05018.

Pang, Y.Z., Wenger, J.P., Saathoff, K., et al., 2009. A WD40 Repeat protein from *Medicago truncatula* is necessary for tissue-specific anthocyanin and proanthocyanidin biosynthesis but not for trichome development. Plant Physiol. 151 (3), 1114–1129.

Passeri, V., Koes, R., Quattrocchio, F.M., 2016. New challenges for the design of high value plant products: stabilization of anthocyanins in plant vacuoles. Front. Plant Sci. 7, 153. https://doi.org/10.3389/fpls.2016.00153.

Payne, C.T., Zhang, F., Lloyd, A.M., 2000. GL3 encodes a bHLH protein that regulates trichome development in *Arabidopsis* through interaction with GL1 and TTG1. Genetics 156 (3), 1349–1362.

Pesch, M., Schultheiß, I., Klopffleisch, K., et al., 2015. TRANSPARENT TESTA GLABRA1 and GLABRA1 compete for binding to GLABRA3 in *Arabidopsis*. Plant Physiol. 168 (2), 584–597.

Pires, N., Dolan, L., 2010. Origin and diversification of basic-helix-loop-helix proteins in plants. Mol. Biol. Evol. 27 (4), 862–874.

Quattrocchio, F., Wing, J.F., Woude, K., et al., 1998. Analysis of bHLH and MYB domain proteins: species-specific regulatory differences are caused by divergent evolution of target anthocyanin genes. Plant J. 13 (4), 475–488.

Ranocha, P., Francoz, E., Burlat, V., Dunand, C., 2014. Expression of *PRX36, PMEI6* and *SBT1.7* is controlled by complex transcription factor regulatory networks for proper seed coat mucilage extrusion. complex transcription factor regulatory networks for proper seed coat mucilage extrusion. Plant Signal. Behav. 9 (11), e977734. https://doi.org/10.4161/15592324.2014.977734.

Schiestl, F.P., Johnson, S.D., 2013. Pollinator-mediated evolution of floral signals. Trends Ecol. Evol. 28 (5), 307–315.

Serna, L., Martin, C., 2006. Trichomes: different regulatory networks lead to convergent structures. Trends Plant Sci. 11 (6), 274–280.

Sievers, F., Wilm, A., Dineen, D., et al., 2011. Fast, scalable generation of high uality protein multiple sequence alignments using Clustal Omega. Mol. Syst. Biol. 7 (7), 1429–1432.

Sobel, J.M., Streisfeld, M.A., 2013. Flower color as a model system for studies of plant evo-devo. Front. Plant Sci. 4 (321). https://doi.org/10.3389/fpls.2013.00321.

Sompornpailin, K., Makita, Y., Yamazaki, M., Saito, K., 2002. A WD-repeat-containing putative regulatory protein in anthocyanin biosynthesis in *Perilla frutescens*. Plant Mol. Biol. 50 (3) 485-195.

Spelt, C., Quattrocchio, F., Mol, J.N.M., Koes, R., 2000. *anthocyanin 1* of petunia encodes a basic helix-loop-helix protein that directly activates transcription of structural anthocyanin genes. Plant Cell 12 (9), 1619–1631.

Stapleton, A.E., Walbot, V., 1994. Flavonoids can protect Maize DNA from the induction of ultraviolet radiation damage. Plant Physiol. 105 (3), 881–889.

Sui, X., Gao, X., Ao, M., et al., 2011. cDNA cloning and characterization of UDP-glucose: anthocyanidin 3-*O*-glucosyltransferase in *Freesia* hybrida. Plant Cell Rep. 30 (7), 1209–1218.

Sun, W., Meng, X., Liang, L., et al., 2015. Molecular and biochemical analysis of chalcone synthase from *Freesia hybrida* in flavonoid biosynthetic pathway. PLoS One 10 (3), e0119054. https://doi.org/10.1371/journal.pone.0119054.

Sun, W., Liang, L., Meng, X., et al., 2016. Biochemical and molecular characterization of a flavonoid 3-*O*-glycosyltransferase responsible for anthocyanins and flavonols biosynthesis in *Freesia hybrida*. Front. Plant Sci. 7 (222), 410. https://doi.org/10.3389/fpls.2016.00410.

Sun, W., Meng, X., Liang, L., et al., 2017. Overexpression of a *Freesia hybrida* flavonoid 3-*O*-glycosyltransferase gene, *Fh3GT1*, enhances transcription of key anthocyanin genes and accumulation of anthocyanin and flavonol in transgenic petunia (*Petunia hybrida*). In Vitro Cell Dev-Pl 53 (5), 478–488.

Taheri, A., Jayasankar, S., Cline, J.A., Raizada, M.N., Pauls, P.K., 2012. A WD-repeat gene from peach (*Prunus persica* L.) is a functional ortholog of *Arabidopsis thaliana TRANSPARENT TESTA GLABRA1*. In Vitro Cell Dev-Pl 48 (1), 23–29.

Tamura, K., Stecher, G., Peterson, D., Filipski, A., Kumar, S., 2013. MEGA6: molecular evolutionary genetics analysis version 6.0. Mol. Biol. Evol. 30 (12), 2725–2729.

Uwagaki, Y., Matsuda, E., Komaki, M., et al., 2015. *Agrobacterium*-mediated transformation and regeneration of *Freesia*×*hybrida*. Plant Biotechnol-Nar 32 (2), 165–168.

Verweij, W., Spelt, C.E., Bliek, M., et al., 2016. Functionally similar WRKY proteins regulate vacuolar acidification in Petunia and hair development in Arabidopsis. Plant Cell 28 (3), 786–803.

Walker, A.R., Davison, P.A., Bolognesiwinfield, A.C., et al., 1999. The *TRANSPARENT TESTA GLABRA1* locus, which regulates trichome differentiation and anthocyanin biosynthesis in *Arabidopsis*, encodes a WD40 repeat protein. Plant Cell 11 (7), 1337–1349.

Wan, H., He, J., Ju, B., et al., 2002. Generation of two-color transgenic zebrafish using the green and red fluorescent protein reporter genes *gfp* and *rfp*. Mar. Biotechnol. 4 (2), 146–154.

Wang, S., Chen, J.G., 2008. Arabidopsis transient expression analysis reveals that activation of *GLABRA2* may require concurrent binding of GLABRA1 and GLABRA3 to the promoter of *GLABRA2*. Plant Cell Physiol. 49 (12), 1792–1804.

Wang, L., Huang, B., He, M., Hao, S., 1990. Somatic Embryogenesis and its hormonal regulation in tissue cultures of *Freesia refracta*. Ann Bot-London 65 (3), 271–276.

Wang, X., Wang, X., Hu, Q., et al., 2015. Characterization of an activation-tagged mutant uncovers a role of GLABRA2 in anthocyanin biosynthesis in Arabidopsis. Plant J. 83 (2), 300–311.

Waters, E.R., 2003. Molecular adaptation and the origin of land plants. Mol. Phylogenetics Evol. 29 (3), 456–463.

Xu, W., Lepiniec, L., Dubos, C., 2014. New insights toward the transcriptional engineering of proanthocyanidin biosynthesis. Plant Signal. Behav. 9 (6), e28736. https://doi.org/10.4161/psb.28736.

Xu, W., Dubos, C., Lepiniec, L., 2015. Transcriptional control of flavonoid biosynthesis by MYB-bHLH-WDR complexes. Trends Plant Sci. 20 (3), 176–185.

Zhao, M., Morohashi, K., Hatlestad, G., Grotewold, E., Lloyd, A., 2008. The TTG1-bHLH-MYB complex controls trichome cell fate and patterning through direct targeting of regulatory loci. Development 135 (11), 1991–1999.

Zhao, H., Wang, X., Zhu, D., et al., 2012. A single amino acid substitution in IIIf subfamily of basic helix-loop-helix transcription factor AtMYC1 leads to trichome and root hair patterning defects by abolishing its interaction with partner proteins in *Arabidopsis*. J. Biol. Chem. 287 (17), 14109–14121.

Zheng, K., Tian, H., Hu, Q., et al., 2016. Ectopic expression of R3 MYB transcription factor gene *OsTCL1* in Arabidopsis, but not rice, affects trichome and root hair formation. Sci. Rep. 6, 19254. https://doi.org/10.1038/srep19254.

Zhou, L., Zheng, K., Wang, X., Tian, H., Wang, X., Wang, S., 2014. Control of trichome formation in *Arabidopsis* by poplar single-repeat R3 MYB transcription factors. Front. Plant Sci. 5, 262. https://doi.org/10.3389/fpls.2014.00262.

Zhu, Z., Wang, H., Wang, Y., et al., 2015. Characterization of the cis elements in the proximal promoter regions of the anthocyanin pathway genes reveals a common regulatory logic that governs pathway regulation. J. Exp. Bot. 66 (13), 3775–3789.

Zohar, B.S., Sylvie, J., Talia, N.H., et al., 2011. A pomegranate (*Punica granatum* L.) WD40-repeat gene is a functional homologue of Arabidopsis *TTG1* and is involved in the regulation of anthocyanin biosynthesis during pomegranate fruit development. Planta 234 (5), 865–881.